Journal of Controlled Release 165 (2013) 101–109

Contents lists available at SciVerse ScienceDirect

Journal of Controlled Release

journal homepage: www.elsevier.com/locate/jconrel

Generation of hypoallergenic neoglycoconjugates for dendritic cell targeted vaccination: A novel tool for specific immunotherapy

Esther E. Weinberger [a], Martin Himly [a], Julia Myschik [b], Michael Hauser [a], Friedrich Altmann [c], Almedina Isakovic [a], Sandra Scheiblhofer [a], Josef Thalhamer [a,*], Richard Weiss [a]

[a] Department of Molecular Biology, University of Salzburg, 5020 Salzburg, Austria
[b] Department of Pharmacy, Pharmaceutical Technology and Biopharmaceutics, Ludwig-Maximilians-University Munich, 81377 Munich, Germany
[c] Department of Biochemistry, University of Natural Resources and Life Sciences, 1190 Vienna, Austria

ARTICLE INFO

Article history:
Received 6 August 2012
Accepted 1 November 2012
Available online 10 November 2012

Keywords:
Targeting
C type lectin receptors
Carbohydrates
Hypoallergen
Specific immunotherapy

ABSTRACT

The incidence of allergic disorders and asthma continuously increased over the past decades, consuming a considerable proportion of the health care budget. Allergen-specific subcutaneous immunotherapy represents the only intervention treating the underlying causes of type I allergies, but still suffers from unwanted side effects and low compliance. There is an urgent need for novel approaches improving safety and efficacy of this therapy. In the present study we investigated carbohydrate-mediated targeting of allergens to dermal antigen-presenting cells and its influence on immunogenicity and allergenicity. Mannan, high (40 kDa) and low (6 kDa) molecular weight dextran, and maltodextrin were covalently attached to ovalbumin and papain *via* mild carbohydrate oxidation resulting in neoglycocomplexes of various sizes. In particular, mannan-conjugates were efficiently taken up by dendritic cells *in vivo* leading to elevated humoral immune responses against the protein moiety and a shift from IgE to IgG. Beyond providing an adjuvant effect, papain glycocomplexes also proved to mask B-cell epitopes, thus rendering the allergen derivative hypoallergenic.
The present data demonstrate that carbohydrate-modified allergens combine targeting of antigen presenting cells with hypoallergenicity, offering the potential for low dose allergen-specific immunotherapy while concomitantly reducing the risk of side effects.

1. Introduction

Targeting antigens to endocytic receptors on antigen presenting cells (APCs) represents an attractive approach to enhance vaccine efficacy. In particular, the mannose receptor (MR) and related C-type lectin receptor (CLR) family members such as DEC205, DC-SIGN, MGL, Langerin, Dectin-1, and Mincle demonstrated excellent carbohydrate antigen-capturing and processing capabilities [1–5]. They are preferentially expressed on APCs, albeit to a type-dependent and varying degree [6]. Particularly immature dendritic cells (DCs) express a large panel of lectins, linked to their important function of sensing and capturing self-, as well as non-self-antigens for processing and presentation onto MHC molecules, thus inducing antigen-specific T-cell activation [7,8]. As pattern recognition receptors, they link innate and adaptive immune responses. Especially the MR has demonstrated effective induction of cellular as well as humoral immune responses, and increased attention is paid to the exploitation of MR- and other CLR-targeted vaccines for cancer, infectious diseases, and for specific tolerance induction in autoimmune diseases [9]. In the present study, we evaluated the immunostimulatory capacity of neoglycoallergens generated by covalent carbohydrate attachment to proteins, and their potential for specific immunotherapy (SIT). SIT represents the only therapeutic intervention for patients suffering from type I allergy, *i.e.* allergic rhinoconjunctivitis, venom hypersensitivity, some drug allergies, or mild bronchial asthma. The most commonly used route of desensitization is subcutaneous immunotherapy (SCIT) by needle injection. SCIT harbors several local and systemic side effects, including urticaria, asthma attacks, and anaphylaxis [10] that vary in incidence from 0.1 to 5% of patients, also depending on the severity of disease [11]. The alarming trend of vastly increasing incidences of allergy and asthma, that already affect about one third of the general population in industrialized countries, requires the development of novel approaches improving the efficacy and decreasing the side effects of SCIT [12].

In the present study, we used mild carbohydrate oxidation for covalent attachment of mannan, a cell wall component of *Saccharomyces cerevisiae*, to ovalbumin (Ova) and papain (Pap). The complex-forming capacities of both proteins were analyzed and compared to other carbohydrate structures, differing in size and origin. The neoglycocomplexes demonstrated excellent DC-targeting potential as assessed by flow cytometric analysis of antigen-loaded DCs in the draining lymph nodes,

* Corresponding author. Tel.: +43 662 8044 5737; fax: +43 662 8044 5751.
E-mail address: Josef.Thalhamer@sbg.ac.at (J. Thalhamer).

0168-3659
http://dx.doi.org/10.1016/j.jconrel.2012.11.002

and induced a significant boost of humoral immunity. Noteworthy, neoglycocomplexes were able to enhance immunogenicity while concomitantly suppressing IgE induction, and proved to be hypoallergenic, an important requirement for safer SCIT.

2. Materials and methods

2.1. Materials

Mannan (MN) from *S. cerevisiae* (average molecular weight approx. 46 kDa), dextran (Dex) from *Leuconostoc mesenteroides* (~40 kDa), dextran from *Leuconostoc* spp. (~6 kDa), and maltodextrin (MD; dextrose equivalent 4.0–7.0, ~3.6 kDa), ovalbumin (Ova) from chicken egg white (grade V), concanavalin A (ConA), protease inhibitor E64, ethylene glycol, sodium borohydride ($NaBH_4$), L-cysteine and sodium periodate ($NaIO_4$) were purchased from Sigma Aldrich (Deisenhofen, Germany). Papain (Pap) from *Carica papaya* was purchased from Roth (Karlsruhe, Germany). Sodium cyanoborohydride ($NaCNBH_3$) was purchased from Fluka Chemie AG (Buchs, Switzerland). pHrodo was obtained from Invitrogen (Darmstadt, Germany). All other reagents were of analytical grade. Pharmacological inactivation of papain using E64 was performed by the addition of 5 mM cysteine-HCl, followed by the addition of E64 in a 100-fold molar excess relative to papain. After 2 h incubation, inactivated papain was dialyzed for removal of excess E64, protein concentrations were calculated by OD_{280} measurement and activity was tested by immunoglobulin cleavage [13].

2.2. Generation of carbohydrate — protein conjugates

Conjugates were generated by an adapted protocol based on a publication of Mislovicova et al. [14]. Briefly, 100 mg of mannan was dissolved in 1 mL (MN1), 2 mL (MN2), 3.5 mL (MN3), or 10 mL (MN4) of an aqueous solution of 50 mM sodium periodate ($NaIO_4$) and vigorously stirred in the dark at 4 °C for 1 h. To stop oxidation, 1 mL ethylene glycol was added and again stirred in the dark for 1 h at 4 °C. Low molecular weight components were then removed from the reaction mixture by dialysis against distilled H_2O at 4 °C in the dark (Spectra/Por dialysis tubing, MWCO 6000–8000, Spectrum Europe B.V., Breda, The Netherlands). The oxidized mannan was then lyophilized and kept at −20 °C. To ensure aldehyde group incorporation, aldehydes were quantified with the amplite colorimetric aldehyde quantitation kit (Biomol, Hamburg, Germany). For protein coupling, the oxidized mannan was reconstituted in 10 mL of a 50 mM sodium phosphate buffer (pH 7) and added to 10 mL of the protein of interest (10 g/L Ova or Pap) dissolved in the same buffer. Additionally, 6 mL of a freshly prepared $NaCNBH_3$ solution (10 g/L in 50 mM sodium phosphate buffer, pH 7) was added and the reaction mixture was kept in the dark and stirred at RT for 24 h. To stop the coupling reaction, 1300 μL of a $NaBH_4$ solution (5 g/L in 50 mM borate buffer, pH 9.5) were added to reduce any remaining aldehyde groups. The reaction was stirred in the dark for 6 h at RT and afterwards dialyzed against H_2O. Protein–carbohydrate conjugates were then lyophilized and kept at −20 °C for long time storage.

To analyze coupling homogeneity, samples were assessed by reducing SDS PAGE (10%) at 140 V for 2 h and stained with a Pro-Q Emerald 300 glycoprotein staining kit (Invitrogen, Carlsbad, CA, USA) for carbohydrate detection, as well as colloidal coomassie for protein visualization. Uncoupled carbohydrates were removed by Vivapure Q Maxi H ion exchange spin columns (Sartorius Mechatronics Austria, Vienna, Austria). Carbohydrate to protein ratio was analyzed by phenol-sulfuric acid method [15] and OD_{280} absorbance, respectively.

2.3. Mannan-binding lectin assay

Carbohydrate integrity was analyzed *via* a precipitation assay using mannan-binding lectin (MBL). In short, 500 μL of increasing amounts of mannan or conjugate [25–400 μg/mL] in assay buffer (50 mM sodium phosphate, 0.1 M NaCl, 0.1 mM $CaCl_2$, 0.1 mM $MnCl_2 \times 4H_2O$, pH 7) were added to 500 μL ConA [230 μg/mL] in assay buffer. The reaction mixtures were stirred at 25 °C for 2 h. Afterwards, samples were centrifuged for 10 min at 8400 *g* and washed twice with 1 mL 1 M NaCl, and the pellet was dissolved in 100 μL 50 mM sodium phosphate (pH 10.5). Turbidity measurement was performed on an Infinite M200 Pro plate reader (Tecan, Salzburg, Austria) at 405 nm in NUNC 96 well plates (Thermo Scientific, Langenselbold, Germany).

2.4. Light obscuration and turbidity measurements

Light obscuration measurements were conducted with a PAMAS-SVSS-C Sensor HCB-LD 25/25 (Partikelmess- und Analysensysteme GmbH, Rutesheim, Germany) to quantify particles ≥ 1 μm. Three aliquots of 0.3 mL of each sample were analyzed. Turbidity was measured by 90° light scattering at λ = 860 nm using a NEPHLA turbidimeter (Dr. Lange, Düsseldorf, Germany). Approximately 1.8 mL of the final samples was analyzed according to the European Pharmacopoeia. The results are reported in formazine nephelometric units (FNU).

2.5. Size exclusion chromatography (SEC) and dynamic light scattering (DLS)

Size-exclusion chromatography was performed using a 26/60 mm Sephacryl S-300 High Resolution column (GE Healthcare, Uppsala, Sweden) on a LC system (pump purchased from Bischoff, Leonberg, Germany; injector type 9125 purchased from Rheodyne, Wertheim-Mondfeld, Germany) equipped with a built-in SunChrom Spectraflow 500 UV–VIS detector (SunChrom, Friedrichsdorf, Germany) for neoglycocomplex size characterization. Samples were analyzed in duplicates using Chromeleon 6.70 SP5. For high-molecular weight MN–Ova preparation, a 10/300 mm Superdex 75 GL column (GE Healthcare, Uppsala, Sweden) on an ÄKTA FPLC chromatography system was employed and data was processed using UNICORN 5.11.

The aggregation behavior in solution was analyzed by dynamic light scattering (DLS802; Viscotek) at 1.2–5 mg/mL for proteins and neoglycocomplexes or 10 mg/mL for carbohydrates in PBS, pH 7 after 10 min centrifugation at 14,000 *g*. Data were accumulated for 10 × 10 s and the correlation function was fitted into the combined data curve, from which the intensity distribution was calculated using solvent settings for water. The calculated intensity distribution was weighted statistically by mass using the mass model for proteins (OmniSizeTM) displaying molecular size R_H (nm) and polydispersity (% RSD) [16].

2.6. Mice and immunizations

Female, 6–10 week-old BALB/c mice were obtained from Charles River Laboratories (Sulzfeld, Germany) and maintained at the animal facility of the University of Salzburg according to the local guidelines for animal care. Animal experiments were performed in accordance with local guidelines approved by the Austrian Ministry of Science (permit number: GZ 66.012/0004-II/10b/2010).

BALB/c mice (n = 5) were immunized intradermally into the ear pinnae with 1 μg Ova, Pap, protease-inactivated Pap (inactivated with E64), or the respective neoglycoantigens (MN–Ova, MN–Pap, Dex–Pap and MD–Pap), dissolved in 80 μL sterile PBS on days 0, 14, and 28. The solution was aliquoted and 40 μL was applied to each of the two pinnae of the animals by needle injection. Blood samples were taken on days 12, 26, and 40. Mice were sacrificed on day 56 when blood samples were taken and splenocytes were prepared. Antibody levels were evaluated *via* a luminometric ELISA assay at indicated serum dilutions lying within the linear range of the assay. Biologically functional IgE was assessed by an *in vitro* basophil release assay and basophil activation assay. Splenocytes were cultured and cellular proliferation by H^3-Thymidin uptake, as well as cytokine secretion upon allergen re-challenge (ELISPOT) was measured. A more detailed description of these assays can be found elsewhere [17].

2.7. Beta-hexosaminidase release from rat basophilic leukemia (RBL) cells

The IgE-crosslinking capacity of the neoglycocomplexes was measured *via* degranulation assay using rat basophil leukemia RBL-2H3 cells. Briefly, RBL-2H3 cells were passively sensitized with IgE-containing sera from Ova- or Pap-sensitized BALB/c mice. After washing, degranulation was triggered by the addition of serial dilutions of the respective neoglycocomplexes, or the unmodified allergens as reference, and beta-hexosaminidase release was measured by enzymatic cleavage of the fluorogenic substrate 4-methylumbelliferyl-N-acetyl-b-D-glucosaminide. Data are expressed as percentage of total release after Triton X-100 treatment [17].

2.8. Basophil activation assay

Basophil activation of murine whole blood samples was analyzed according to Torrero et al. [18]. Whole blood (50 μL) was diluted with 50 μL RPMI 1640 (PAA, Pasching, Austria) containing 200 μg/mL heparin, and incubated with 40 μg/mL of the respective antigen (Ova or E64-inactivated Pap), with 2 μg/mL anti-IgE (clone 23G3, eBioscience) as positive control, or left untreated as negative control for 2 h at 37 °C and 7% CO_2. Cells were washed and centrifuged at 500 *g* for 5 min prior to surface staining using anti-CD200R3 (clone Ba103, Hycult biotech), anti-CD49b (clone DX5, BioLegend), anti-CD200R (clone OX110, eBioscience), and anti-CD45 (clone 30-F11, BD biosciences). After incubation, cells were washed twice with PBS/1%BSA/2 mM EDTA and analyzed on a FACSCanto II flow cytometer using FACSDiva Software (BD Biosciences).

2.9. Flow cytometric analysis and histology of antigen-loaded draining lymph node DCs

Mice were immunized intradermally into the ear pinnae with 50 μg pHrodo-labeled antigen (Ova, Pap, MN–Ova, MN–Pap or Dex–Pap) dissolved in 20 μL sterile PBS. The solution was aliquoted and 10 μL was applied to each of the two pinnae of the animal. 24 h later, antigen uptake and transport to the ear-draining lymph nodes (dLNs) by resident DCs were characterized by FACS analysis. Pinna-dLN nodes were prepared [19], pooled for each group and surface stained using anti-MHCII (clone M5/114, BD Pharmingen), anti-CD11b (clone M1/70, BioLegend), anti-CD11c (clone N418, eBioscience), and anti-CD8α (clone 53-6.7, eBioscience). For fluorescent microscopy, mice received 10 μg pHrodo-labeled MN–Ova into the ear pinna and dLNs were excised 30 min after injection. LNs were treated with 1% PFA in PBS for 10 min, then placed in OCT compound (Tissue-Tek) and frozen in liquid nitrogen. 8 μm sections were sliced on a Cryostat microtome. Sections were rehydrated in PBS and stained with 1 μg/mL Hoechst 33242 dye (Invitrogen) for 10 min. After washing, sections were coverslipped with Roti®-Mount FluorCare (Carl Roth).

2.10. Antigen uptake analysis using bone marrow derived dendritic cells (BMDCs)

BMDC precursors were harvested from femurs/tibias and were cultured in RPMI 1640 complete medium (10% FBS, 2 mM L-glutamine, 10 ng/mL GM-CSF, 100 U/mL penicillin, 0.1 mg/mL streptomycin). At day 3, 50% of medium was replaced. At day 7, BMDCs were harvested and stored frozen until further use. BMDCs were thawed and placed in complete medium in 96-well polystyrene V-bottom plates (Greiner) for 2 h. 10^5 cells per well were treated with 30, 10, 3.3, 1.11 and 0 μg/mL pHrodo-labeled antigen (Ova, Pap, MN–Ova or MN–Pap) and uptake was analyzed 10, 30 and 60 min later by flow cytometry. BMDCs were additionally surface-stained with anti-MHCII (clone M5/114, BD Pharmingen), anti-CD86 (clone GL1, BioLegend), anti-CD40 (clone HM40-3, eBioscience).

To visualize antigen uptake by fluorescence microscopy, BMDCs were incubated on 8-well cell culture slides (PAA) in complete medium treated with 20 μg/mL pHrodo–MN–Ova for 1 h, centrifuged and then fixed with 1% PFA in PBS for 10 min. After washing, cellular nuclei were again stained with 1 μg/mL Hoechst dye for 10 min.

2.11. Statistical analysis

Statistical significance between groups was assessed by Students *T*-Test using SigmaStat 2.0 or GraphPad Prism 5.01.

3. Results

3.1. Preparation of neoglycoantigens

Carbohydrate polymer coupling to protein antigens requires the partial oxidation of the carbohydrate to generate reactive aldehyde groups for covalent attachment to amine-containing molecules. Briefly, the carbohydrate polymer is oxidized with sodium periodate and the newly generated aldehyde groups are used for covalent attachment to the protein's lysines and 5′amine groups by reduction with cyanoboroanhydride. The efficacy of aldehyde incorporation upon mannan oxidation was analyzed and displayed a linear correlation of incorporated aldehyde groups with the amount of sodium periodate used (Supplementary Fig. S1). As this procedure requires the structural disruption of single carbohydrate monomers in the mannan polymer, the oxidized carbohydrates were analyzed for structural integrity by specific interaction with ConA, a specific mannan-binding lectin (Fig. 1A). Oxidized mannans MN1–MN3 displayed a precipitation curve comparable to mannan, whereas a higher degree of oxidation (MN4) resulted in complete disruption of the carbohydrate structure as indicated by a weak ConA interaction, leaving MN1–MN3 as candidates for further analysis.

The efficiency of MN1–MN3 to bind to the protein antigens Ova and Pap was evaluated using a denaturing SDS-PAGE stained with coomassie for protein detection (Fig. 1B and E) and Pro-Q Emerald 300 glycoprotein stain for carbohydrate visualization (Fig. 1C and F). Increased oxidation of mannan led to increased coupling efficacy for all proteins tested, but the overall quantitative turnover was strongly dependent on the protein. Whereas coupling of MN1–MN3 to Ova resulted in partial quantitative conjugation to the proteins (Fig. 1A, B and C), conjugation to papain led to a complete quantitative turnover of the protein with MN3 (Fig. 1E and F). Mannan–papain conjugates barely entered the resolving gel, while the small fraction of mannan–ovalbumin complexes showed a smear up to over 250 kDa. This heterogeneity may mirror the Gaussian distribution of the carbohydrate size obtained from natural source. Furthermore, especially highly glycosylated proteins display an aberrant migratory behavior on SDS-PAGE, because carbohydrates do not bind SDS and the resulting decreased charge-to-mass ratio of the protein–SDS complex leads to an increased apparent molecular weight (MW) [20]. The shape of denatured glycoproteins is also hardly comparable to the partly unglycosylated sizing standards that contributes additionally to aberrant MW estimates.

3.2. Characterization of MN–Ova and MN–Pap

Based on coupling efficacy and carbohydrate integrity analysis using ConA precipitation, Ova- and Pap-conjugates with periodate-oxidized mannan MN3 were chosen for further analysis and designated MN–Ova and MN–Pap. As MN–Ova contained a significant amount of unconjugated protein according to the SDS-PAGE data, the samples were subjected to HPLC using a superdex G75 column for high-MW conjugate separation. Analysis of Ova revealed two peaks, a major peak at 37 min, and a small one at 32 min. Coupling of mannan to Ova left most of the protein unmodified, but led to a

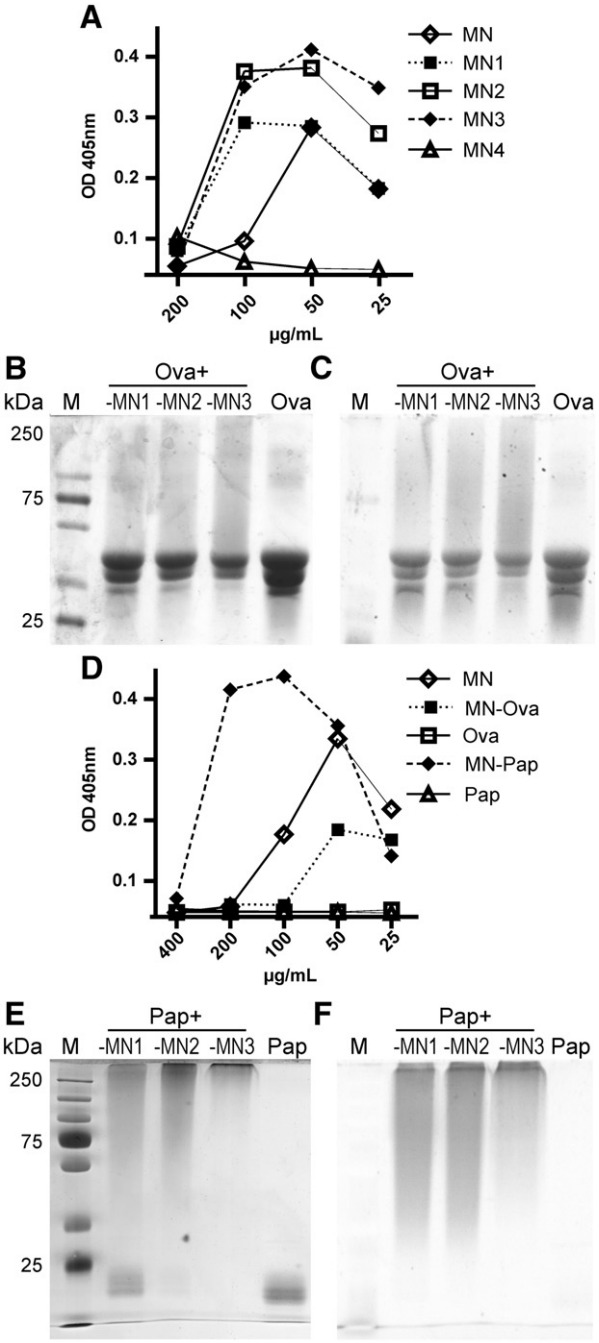

G

Samples	Protein content [µg]	Carbohydrate content [µg]	Index Carb./Prot.
Pap	50	18.5 ± 0.5	0.37
MN	-	-	-
MN-Pap	50	38.3 ± 0.5	0.77
Ova	25	0.9 ± 0.02	0.03
MN-Ova	25	27.0 ± 0.8	1.2

Samples	Rh [nm]	% RSD	>450 kDa	450-120 kDa	120-43 kDa
Pap	2.2 ± 0.37	16.6	-	-	-
MN	4.5 ± 1.4	31.6	-	-	-
MN-Pap	19.6 ± 4.6	23.9	67%	30%	3%
Ova	-		-	-	-
MN-Ova	-		7%	38%	55%

broadened small peak at around 32 min (Supplementary Fig. S2A). Sample fractions 4–10, containing high-MW MN–Ova conjugates were pooled (Supplementary Fig. S3).

The generation of MN–Pap, using periodate-oxidized mannan MN3 resulted in total conversion of Pap used in the reaction, making further purification steps negligible. At last, both neoglycocomplexes were separated from unbound mannan by anion exchange chromatography.

To evaluate homogeneity of the samples after purification, size characterization was performed *via* SEC on a Sephacryl S-300 High Resolution column and DLS; and the ratio of protein to carbohydrate content in the complexes was assessed (Fig. 1G). SEC data matched SDS-PAGE data and confirmed the heterogeneity of the neoglycocomplexes. While the majority (67%) of MN–Pap was composed of complexes over 450 kDa, MN–Ova contained complexes ranging predominantly from 45 kDa up to 120 kDa (55%). DLS confirmed the high-MW nature of MN–Pap (Rh = 19.5 ± 4.5 nm), but did not allow for precise MW estimates, due to the complex carbohydrate–protein content. To evaluate whether covalent attachment of proteins still allowed for structural mannan recognition, the newly generated neoglycoantigens were subjected to ConA precipitation (Fig. 1D). MN–Ova and MN–Pap still displayed specific interaction with ConA, proving the integrity of carbohydrates in the complex.

3.3. Impact of carbohydrate variability on neoglycoantigen formation

The impact of carbohydrate variability on neoglycoantigen formation was assessed by analyzing three additional carbohydrates that differ in size and origin for their potential to form complexes with Ova and Pap. Mannan (48 kDa) was compared to two dextrans (40 kDa [Dex40] and 6 kDa [Dex6]) derived from *P. leuconostoc* and maltodextrin (3.6 kDa), a common food additive. Carbohydrate preparation was performed according to the protocol established for mannan, and the oxidation rate of MN3 was also applied to the other carbohydrates. After covalent coupling, neoglycocomplexes were again analyzed on a SDS-PAGE (Fig. 2B and E).

Complex-forming capacity demonstrated to be an inherent feature of the engaged protein molecule. Again, Ova displayed low complex-forming capacity with all carbohydrates tested, while Pap-neoglycoconjugates were all of high-MW (Fig. 2B and E). Coupling dextran (6 kDa) to papain (Dex6–Pap) resulted in precipitation of neoglycocomplexes that could not be loaded onto SDS-PAGE. Instead, the supernatant was loaded, which contained only a small percentage of soluble low-MW complexes (Fig. 2B). Particle formation analysis using turbidity measurements (Fig. 2C) and light obscuration (Fig. 2D) revealed elevated FNU levels for Dex6–Pap, which are indicative for partial particle formation. Light obscuration confirmed formation of particles of >25 µm. Pap-neoglycocomplexes were further subjected to DLS and SEC analyses and the carbohydrate content was evaluated using the phenol-sulfuric acid method [15] (Fig. 2A). In comparison to papain, the R_H of the MN–Pap complex increased up to 9-fold (Fig. 1G) and that of MD–Pap and Dex40–Pap doubled (Fig. 2A). SEC confirmed size distribution of the Pap-neoglycocomplexes (Fig. 2A).

Fig. 1. Analysis of mannan-protein neoglycocomplexes. A) The structural integrity of mannan after functionalization and (D) in neoglycocomplexes of papain (Pap) or ovalbumin (Ova) was evaluated *via* ConA precipitation: Increasing doses (x-axis) of mannan (MN), its oxidized derivatives (MN1–MN4), or antigen (MN–Ova, Ova, MN–Pap, Pap) were added to ConA [230 µg/mL] and OD was measured at 405 nm. Increasingly oxidized mannans (MN1–MN3) were covalently attached to Ova (B and C) generating MN–Ova (Ova + MN1–MN3) or Pap (E and F) generating MN–Pap (Pap + MN1–MN3) and separated by SDS PAGE visualizing protein (B and E) and carbohydrate (C and F) content. M = molecular weight size marker. G) shows a table depicting the protein and carbohydrate content in the neoglycocomplexes and their indices (carbohydrate/protein) analyzed *via* OD_{280} and phenol-sulfuric acid method [15], respectively. DLS evaluated R_H and %RSD; and the size distribution was assessed by SEC using a Sephacryl S-300 High Resolution column. Size distribution was calculated in percentage from area under curve of obtained chromatograms and sizing was categorized in 120–43 kDa, 450–120 kDa and >450 kDa.

A

Samples	Protein content [µg]	Carbohydrate content [µg]	Index Carb./Prot.
Pap[1]	50	7.1 ± 0.02	0.14
MD[1]	-	-	-
MD-Pap[1]	50	10.9 ± 0.08	0.22
Pap[2]	50	22.9 ± 0.03	0.46
Dex40[2]	-	-	-
Dex40-Pap[2]	50	45.7 ± 0.3	0.91

Samples	Rh [nm]	% RSD	>450 kDa	450-120 kDa	120-43 kDa	<43 kDa
Pap[1]	2.2 ± 0.37	16.6	-	-	-	-
MD[1]	4.4 ± 1.99	45.4	-	-	-	-
MD-Pap[1]	5.0 ± 1.96	39.2	15%	42%	23%	20%
Pap[2]	2.2 ± 0.37	16.6	-	-	-	-
Dex40[2]	4.7 ± 1.67	35.5	-	-	-	-
Dex40-Pap[2]	5.1 ± 2.02	39.8	11%	48%	28%	13%

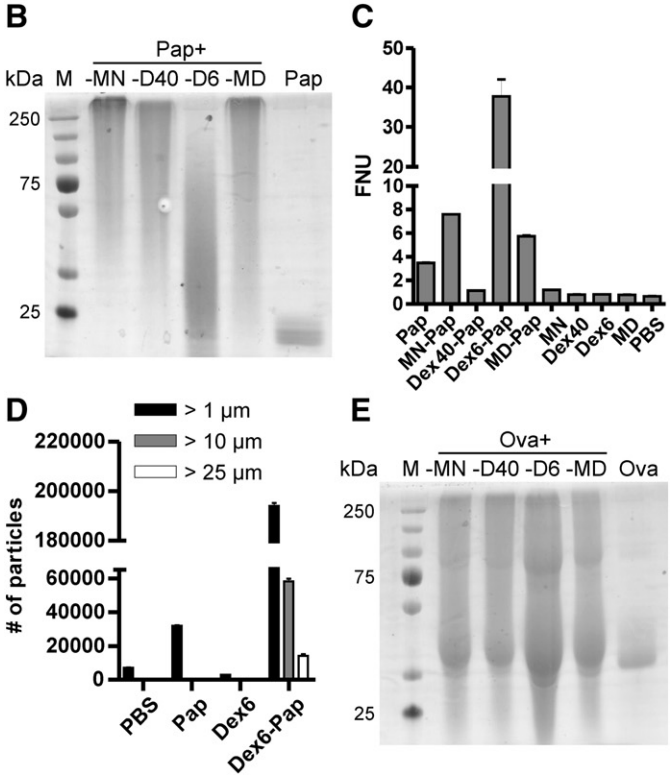

Fig. 2. Influence of carbohydrate variability on neoglycocomplex formation. Panel A depicts a table of the protein and carbohydrate content in MD–Pap and Dex40–Pap and their indices (carbohydrate/protein). R_H and %RSD were analyzed *via* DLS and size distribution was assessed by SEC. Functionalized dextrans (D40 and D6) and maltodextrin (MD) were conjugated to Pap (B) or Ova (E), separated, and coomassie stained on a denaturing SDS-PAGE. Dex6–Pap was further subjected to turbidity measurements (C) and light obscuration (D).

Enzymatic activity of papain after carbohydrate attachment was tested by proteolytic IgG digest (Supplementary Fig. S1A). In comparison to unmodified papain activated with (Pap+) or without 5 mM L-cysteine (Pap−), neoglycocomplexes displayed reduced (MD–Pap and D40–Pap) or no proteolytic activity (MN–Pap).

Due to the small percentage of generated Ova-neoglycocomplexes, only MN–Ova has been chosen for further *in vivo* analysis after SEC preparation.

3.4. Mannan-neoglycoantigens are efficiently taken up by resident DCs

We addressed the question whether carbohydrate coupling increased antigen uptake by DCs *via* C-type lectin receptor targeting. Therefore, the antigens were labeled with pHrodo Red dye (Invitrogen), a dye that specifically fluoresces as pH decreases from neutral to acidic, as provided in endosomes/lysosomes of cells. *In vitro* characterization of the cellular uptake of neoglycocomplexes using bone marrow derived dendritic cells (BMDCs) demonstrated superior ingestion of mannan-conjugates MN–Ova and MN–Pap (Supplementary Fig. S4A-D,F). This was confirmed *in vivo* by intradermal needle-injection of labeled antigen into the ear pinnae of mice. Antigen uptake and transport to the ear dLNs were measured after 24 h by FACS analysis. DCs in cervical LNs were identified according to their high expression of MHC class II (Fig. 3A) and additionally characterized by CD8α, CD11b, and CD11c expression and uptake of pHrodo-labeled antigen (Fig. 3B, D–F). The results showed significantly elevated numbers of pHrodo + $MHCII^{high}$ DCs for mannan conjugates MN–Ova and MN–Pap (and to a lesser degree for MD–Pap) in comparison

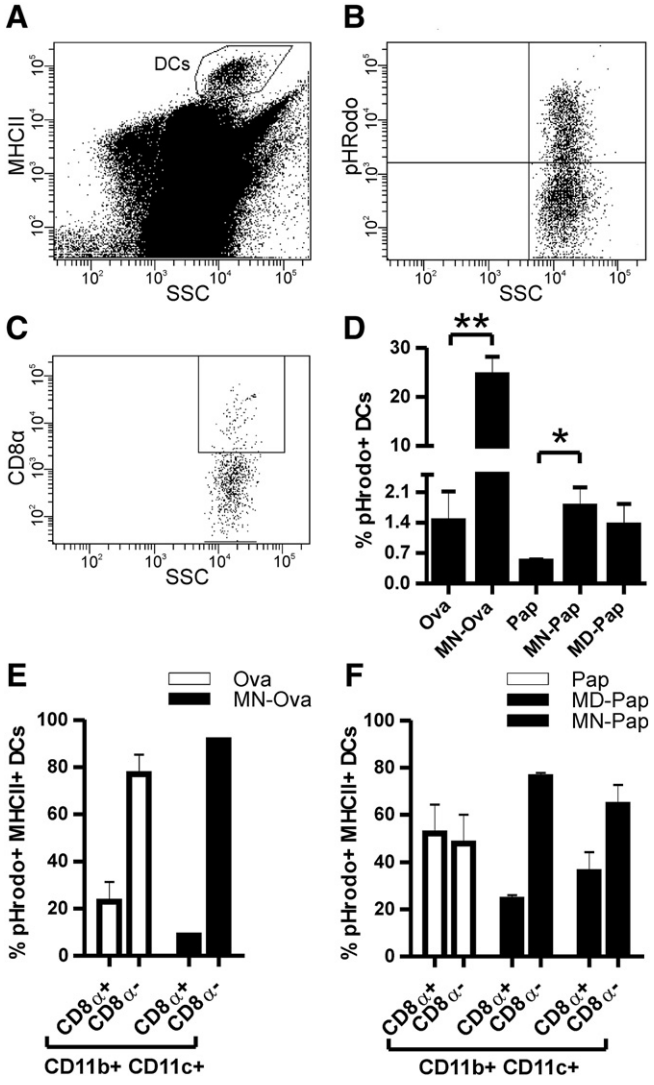

Fig. 3. Analysis of DCs in cervical dLNs 24 h after intradermal injection of pHrodo-labeled neoglycocomplexes *vs.* unmodified allergens into the mouse ear pinnae. Gating strategy to identify MHC-II^{high} DCs (A), further characterized into CD8α positive and negative DCs (D) as well as quantitation of (here depicted MN–Ova) pHrodo+ DCs (B). Percentage of MHC-II^{high} and pHrodo+ DCs in dLNs (C). DC subclass distribution of pHrodo+ DCs in dLNs (E and F). Data are shown as means ± SEM (n = 3). * $P<0.05$; ** $P<0.01$.

to the unmodified antigens (Fig. 3C). Both carbohydrates targeted antigen preferentially to CD8α− DCs, as indicated by an increase in CD8α−/pHrodo+ DCs compared to unmodified antigens (Fig. 3E and F). Nevertheless, whether the antigens were taken up *in situ* by dermal DCs or by LN resident APCs *via* the afferent lymphatics could not be fully elucidated. Histology revealed that antigen-loaded cells in the dLNs were already present 30 min after intradermal injection (Supplementary Fig. S4G), suggesting both mechanisms.

3.5. Neoglycoantigens display elevated immunogenicity in vivo while reducing the IgE-inducing capacity

In order to test the efficacy of neoglycoantigens to trigger immunity *in vivo*, we targeted dermal DCs in the ear pinnae of mice by intradermal injection of low dose antigen. For this purpose, we selected the optimal candidate from *in vitro* studies, *i.e.* mannan-conjugates.

In two independent experiments (Fig. 4), we confirmed the data of the *in vitro* studies. Mannan-neoglycoconjugates MN–Ova and MN–Pap displayed superior induction of papain-specific IgG antibodies, as compared to Ova or Pap-immunized animals (Fig. 4A–D). Antibody subclass analysis revealed a predominance of IgG1 (data not shown). While boosting immunogenicity, neoglycocomplexes concomitantly reduced the allergenicity of the respective allergen, with mannan conjugates showing the lowest induction of IgE responses (Fig. 4E and F).

Although immunization with MN–Ova induced no circulating antigen-specific IgE as detected by the RBL assay (Fig. 4E), flow cytometric analysis of blood basophils *via* basophil activation test revealed similar levels of cell bound IgE compared to the unconjugated antigen (Supplementary Fig. S5E). In contrast, the reduced IgE levels detected after immunization with MN–Pap (Fig. 4F) could also be confirmed on basophils (Supplementary Fig. S5F).

While humoral immunity was clear-cut at the low antigen dosage tested, systemic immune responses, as analyzed with spleen cells, were too weak to elicit measurable results (data not shown).

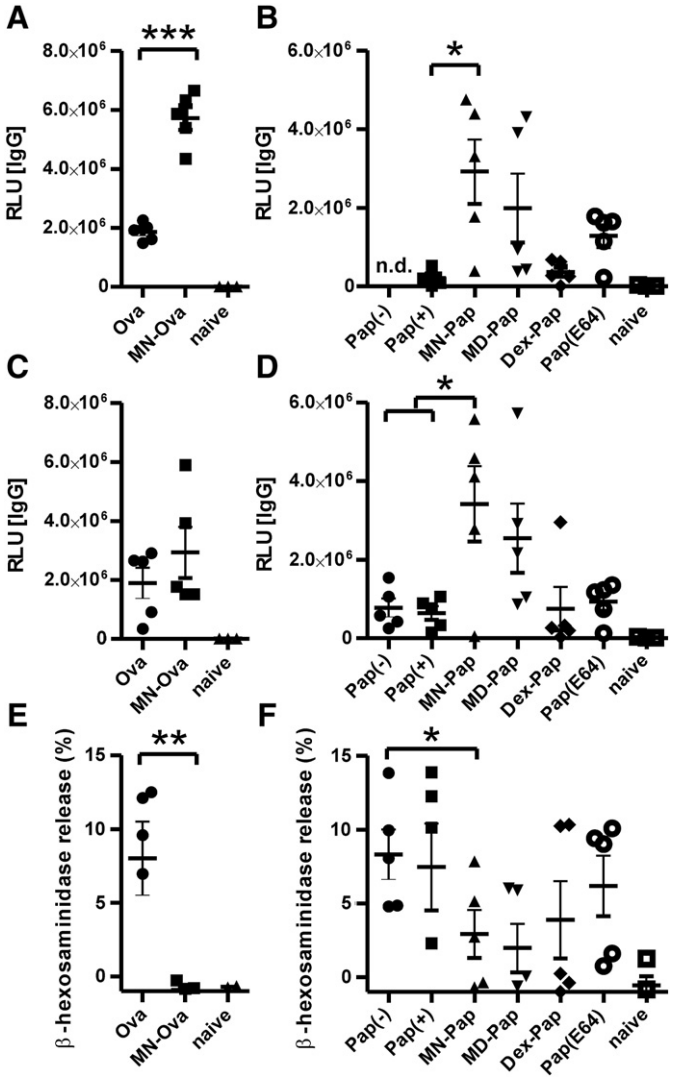

Fig. 4. Humoral immune profile after intradermal immunization of BALB/c mice with neoglycocomplexes. A–D) Allergen-specific IgG two weeks after the last immunization was analyzed *via* ELISA. Two individual experiments are shown (experiment 1 — A and B, experiment 2 — C–F). E and F) Biologically functional IgE of experiment 2 was assessed by RBL assay. Serum dilutions were 1:100 for IgG and 1:17 for IgE. Data are shown as individual data points (n = 3–5). * $P<0.05$; ** $P<0.01$; *** $P<0.001$.

3.6. Carbohydrate conjugates of papain are hypoallergenic

The potential of neoglycoantigens to trigger immediate phase immune responses was analyzed by IgE-mediated degranulation of RBL cells upon allergen encounter *in vitro*. RBL cells were incubated with mouse sera containing high levels of allergen-specifc IgE. The concentrations of neoglycoantigens *vs.* unmodified antigens to induce 10% of maximal degranulation were determined by titrations (Fig. 5A and B), and the reduction of allergenic potential was calculated by dividing the effective concentration of the neoglycoantigen by that of the unmodified antigen. Whereas MN–Ova showed no difference in β-hexosaminidase release compared to unmodified Ova (1.1-fold reduction), Pap-neoglycocomplexes displayed an up to 1600-fold reduction for MN–Pap, 104-fold for Dex40-Pap, and 21-fold for MD–Pap.

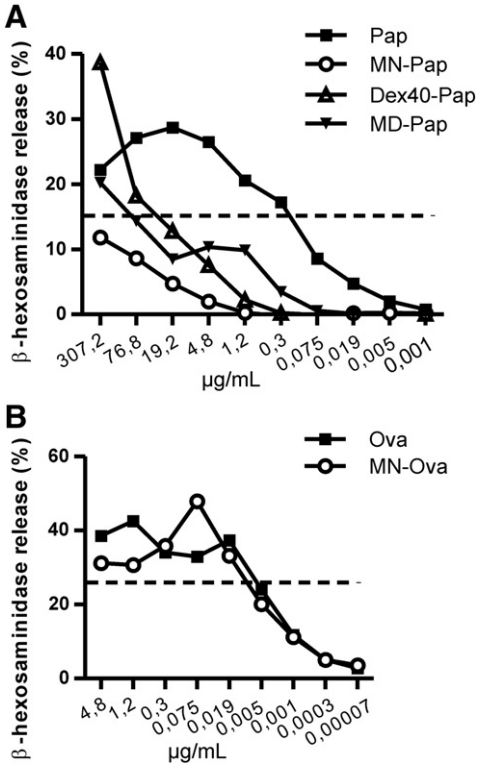

Fig. 5. Hypoallergenicity of carbohydrate coupled antigens. IgE-sensitized RBL cells were stimulated with increasing concentrations of Ova (A) or Pap (B) antigens *vs.* neoglycoantigens, and β-hexosaminidase release curves were compared at the 10%-release log-phase of the Gaussian release curve.

4. Discussion

Targeting antigens to DCs *via* addressing specific DC surface molecules demonstrated great potential for enhancing vaccine efficacy [21]. DCs are sentinels and indispensable key players in both, the initiation and polarization of immune responses, either promoting tolerance or an appropriate form of immunity [21]. Meanwhile, DCs have been tested for cancer immunotherapy, using re-infusion of *in vitro*-generated DCs loaded with tumor antigen [22]. However, recent advances favor a much simpler and versatile approach by delivering antigens directly to DCs *in situ* [23].

Interesting targets on DCs are receptors of the innate immune surveillance system that mediate the recognition and uptake of antigens, such as CLR family members (also known as endocytic receptors or antigen-uptake receptors) [6,24]. These receptors have been demonstrated to be responsible for the recognition and internalization of glycosylated self- and foreign antigens, thus leading to antigen presentation on both MHC class I and II molecules.

The present study evaluated the feasibility of carbohydrate-mediated targeting of allergens to dermal APCs in terms of immunogenicity and allergenicity as potential candidates for SCIT.

We largely focused on mannan, an approximately 48 kDa surface carbohydrate polymer derived from *S. cerevisiae*, which was covalently conjugated to the model allergens Ova and Pap. Mannan and mannose units have already been successfully used to generate more efficient immune responses against attached ligands in animal models as well as in human clinical trials [25–27]. In our study, mannan was functionalized by reactive aldehyde incorporation *via* controlled and mild periodate oxidation followed by covalent attachment to the protein's amine groups [14] to generate high-MW conjugates. A huge body of evidence clearly demonstrated a link between protein antigen formation and the propensity to trigger immunity. Especially high-MW arrays of protein antigens (multimers > 100 kDa) elicited superior humoral immune responses in comparison to their low-MW, non-aggregated monovalent form [28]. In this context, multimerization is the key to immunogenicity, most probably by mimicking repetitive microbial "patterns" to which our immune system has evolved [29]. Here, we utilized the potential of oxidized mannan and other carbohydrates to act as multifunctional crosslinking agents, not only to facilitate C-type lectin receptor targeting of our antigenic information, but also to take advantage of the immunogenicity-enhancing properties of protein aggregates.

Coupling efficacy turned out to be strongly influenced by the degree of oxidation of the functionalized carbohydrate, as well as by the antigenic nature of the protein molecule (Fig. 1), leading to large and total quantitative complex formations for Pap, and to small and considerably less complex formation for Ova. The integrity of the carbohydrate and of functional B-cell epitopes was maintained as shown in Figs. 1 and 4. Coupling efficacy was mainly determined by the protein antigen, as three other carbohydrate molecules varying in origin and size, including two dextrans from gram-positive *Leuconostoc* spp. (40 kDa and 6 kDa) and the common food additive maltodextrin (3,6 kDa) also showed weaker coupling efficacy to Ova than to Pap. However, the carbohydrate moiety had an impact on the size distribution of the resulting complexes (Fig. 2A, B and E).

Coupling of dextran (6 kDa) to papain even resulted in the formation of microparticles of > 25 μm, as demonstrated by light obscuration (Fig. 2C and D). Partial precipitation of these particles impaired accurate protein quantification, which would be a necessary prerequisite for *in vivo* applications. Therefore, this conjugate was excluded from further experiments.

The observed heterogeneity of complex formation, especially for papain conjugates, could be due to intramolecular disulfide re-bonding upon re-oxidation after carbohydrate coupling and aldehyde quenching. While Ova harbors one disulfide bond at amino acids (AA) 74–121, papain carries three (AA155–196, 189–228, and 286–333), and this may add up to the excellent complex-forming capacity of papain under the engaged coupling conditions. As covalent attachment of carbohydrate molecules potentially causes sterical hindrance of the enzymatic activity of papain, we compared the proteolytic activity of papain to that of the neoglycoantigens by rat IgG digest (Supplementary Fig. S1). Carbohydrate attachment to papain strongly diminished (MD–Pap and Dex40–Pap) or even abrogated (MN–Pap) its proteolytic activity.

In an *in vivo* approach we analyzed the ability of neoglycoantigens to trigger immune responses after intradermal injection. Mannan-conjugation resulted in strongly elevated numbers of antigen-loaded DCs in dLNs (Fig. 3C and Supplementary Fig. S4G). Engaging mannan in this context may be superior to other carbohydrate structures as it targets a variety of mannose receptors such as MR, DC-SIGN and possibly other PPRs [9]. Further *in vitro* antigen uptake characterization using BMDCs (Supplementary Fig. S4A-D,F) substantiated our hypothesis of the superior APC targeting potential and is in accordance with former publications demonstrating improved processing and presentation of mannosylated antigens by DCs [2,30].

The pattern of CLR expression varies among the different functional DC subpopulations [6]. We therefore performed FACS analysis which revealed that the majority of antigen-loaded DCs were CD8α− CD11b+CD11c+, a subset belonging to the "myeloid" lineage of DCs [31]. Myeloid DCs are also known as conventional DCs and are, apart from plasmacytoid DCs, one of the two main subsets found in mice [31]. Certain DC subsets seem to play an important role in the induction of allergic inflammation and asthma, possibly through their ability to direct the development of distinct T helper cell populations [32]. While CD8α+ cells are prone to induce Th1 differentiation, CD8α− cells preferentially trigger a Th2 response [33–35]. However, the polarizing capacities of these DC subsets are not clear-cut and myeloid CD8α− DCs have also been demonstrated to produce IFN-γ and therefore can trigger a Th1-biased immune response under conditions of intense immune stimulation such as bacterial or viral infections [36,37].

Intradermal immunization with neoglycoantigens also resulted in enhanced humoral immune responses (Fig. 4A–D), with MN–Ova and MN–Pap showing the strongest effects. CLRs demonstrated both, to induce tolerance [38–40] as well as to enhance immunogenicity in a context-dependent manner for various infectious diseases and cancer [9]. Antibody responses measured in these studies were predominantly of the IgG1 subtype. This is in agreement with our data, as we could not detect IgG2a antibodies in any group indicating that CLRs do not promote Th1 polarization in this setting.

With respect to their applicability for allergy immunotherapy, neoglycoantigens combine two important features, *i.e.* improving the immunogenicity and decreasing the allergenic potential of the protein part of the conjugate (Fig. 4E and F). In this context, we define the allergenicity of a molecule as the potential to induce a Th2-type response, resulting in IgE production. This effect is most obvious for mannan-conjugates that induced significantly decreased IgE responses against the unmodified allergen. To more closely investigate the IgE-inducing capacity of our neoglycocomplexes, we isolated basophils from the blood of immunized animals and determined their activation status (CD200R up-regulation) upon allergen re-encounter (Supplementary Fig. S5). Contrasting the RBL data (Fig. 4E), MN–Ova immunization did not lead to a diminished activation of circulating basophils upon Ova encounter, while MN–Pap again lacked basophil IgE-sensitizing capacity, comparable to that of naïve animals. While in the RBL assay, non-cell-bound allergen-specific IgGs are washed away before addition of antigen, which cross-links IgE, antigen stimulation of basophils during the basophil activation test takes place in whole blood samples. Therefore, blocking IgG induced by the vaccination can interfere with cross-linking of basophil-bound IgE in this assay, a phenomenon well known from allergen-specific immunotherapy [41]. Furthermore, neoglycoantigens also can be considered as hypoallergens in the context of binding to pre-existing IgE antibodies, which is a major source of side effects during

SIT. In our study, again MN–Pap proved to be the most efficient hypoallergen, as could be measured with an *in vitro* IgE-mediated RBL degranulation assay (Fig. 5A and B), which resulted in a 1600-fold reduction of IgE binding to the conjugate. Although this effect may be attributed to the protective masking effect of the carbohydrate moieties in the high MW complexes of Pap-neoglycocomplexes, it is intriguing that at the same time, MN–Pap is a potent inducer of IgG responses (Fig. 4B and D). Recent findings suggest that IgM+ naïve B cells directly switch to IgE+ B cells and that IgG1 memory B cells are not a major source for IgE (*i.e.* they do not switch to IgE after secondary antigen encounter) [42], although sequential class switching from IgG1 to IgE may be required for the generation of high affinity IgE antibodies [43]. However, this topic is still controversially discussed (also see [44]). While, immature B cells have been shown to preferentially class-switch to IgE rather than IgG [45], He et al. have shown that B cells directly stimulated through CLRs in the absence of T cell help can induce class switch to IgG and IgA [46]. Together, these findings provide a mechanistic insight in how application of neoglycoconjugates may switch the humoral immune profile from IgE to IgG.

Summing up, our data show that covalent attachment of carbohydrates to proteins results in complex-formation of various sizes, depending on the nature of the antigen as well as the carbohydrate molecule. The coupling procedure leads to heterogeneous coupling results for the engaged proteins and future studies will investigate which size range and carbohydrate to protein ratio are optimal for SIT application, in order to create individualized and protein tailored coupling protocols. The coupling protocol leaves room for variation, *e.g.* optimization of Schiff's base formation *via* pH alteration and milder aldehyde quenching conditions using ethanolamine.

Complex formation can reduce the enzymatic activity and IgE binding capacity of the molecules and can switch the induced antibody profile from IgE to IgG, but again these effects depend on antigen and carbohydrate. The reduced IgE binding capacity of neoglycoprotein conjugates make these molecules interesting candidates for therapeutic application in allergic diseases with improved immunogenicity and safety. It is known that a successful therapeutic outcome in allergy treatment is associated with high dose allergen regimes [47], therefore, hypoallergenicity is a major requirement to improve the safety of allergy vaccines [48]. Especially, tailored DC targeting with mannan conjugation to antigens represents an interesting approach for future immunotherapy, allowing the application of lower allergen dosages and lowering the risk of side effects.

Acknowledgments

This work was supported by the Austrian Science Fund, project #W1213, the Christian Doppler Research Association, and by Biomay AG, Vienna, Austria. None of the funding institutions were involved in study design, the collection, analysis and interpretation of data, in the writing of the report, or in the decision to submit the article for publication. Special thanks go to Dr. Günter Schwamberger for critically discussing carbohydrate coupling techniques and to Thomas Dalik for advice on SEC matrices.

Appendix A. Supplementary data

Supplementary data to this article can be found online at http://dx.doi.org/10.1016/j.jconrel.2012.11.002.

References

[1] A. Engering, T.B. Geijtenbeek, S.J. van Vliet, M. Wijers, E. van Liempt, N. Demaurex, A. Lanzavecchia, J. Fransen, C.G. Figdor, V. Piguet, Y. van Kooyk, The dendritic cell-specific adhesion receptor DC-SIGN internalizes antigen for presentation to T cells, J. Immunol. 168 (2002) 2118–2126.
[2] A.J. Engering, M. Cella, D. Fluitsma, M. Brockhaus, E.C. Hoefsmit, A. Lanzavecchia, J. Pieters, The mannose receptor functions as a high capacity and broad specificity antigen receptor in human dendritic cells, Eur. J. Immunol. 27 (1997) 2417–2425.
[3] K. Mahnke, M. Guo, S. Lee, H. Sepulveda, S.L. Swain, M. Nussenzweig, R.M. Steinman, The dendritic cell receptor for endocytosis, DEC-205, can recycle and enhance antigen presentation via major histocompatibility complex class II-positive lysosomal compartments, J. Cell Biol. 151 (2000) 673–684.
[4] M.M. Weck, S. Appel, D. Werth, C. Sinzger, A. Bringmann, F. Grunebach, P. Brossart, hDectin-1 is involved in uptake and cross-presentation of cellular antigens, Blood 111 (2008) 4264–4272.
[5] C.A. Wells, J.A. Salvage-Jones, X. Li, K. Hitchens, S. Butcher, R.Z. Murray, A.G. Beckhouse, Y.L. Lo, S. Manzanero, C. Cobbold, K. Schroder, B. Ma, S. Orr, L. Stewart, D. Lebus, P. Sobieszczuk, D.A. Hume, J. Stow, H. Blanchard, R.B. Ashman, The macrophage-inducible C-type lectin, mincle, is an essential component of the innate immune response to Candida albicans, J. Immunol. 180 (2008) 7404–7413.
[6] C.G. Figdor, Y. van Kooyk, G.J. Adema, C-type lectin receptors on dendritic cells and Langerhans cells, Nat. Rev. Immunol. 2 (2002) 77–84.
[7] L.C. Bonifaz, D.P. Bonnyay, A. Charalambous, D.I. Darguste, S. Fujii, H. Soares, M.K. Brimnes, B. Moltedo, T.M. Moran, R.M. Steinman, In vivo targeting of antigens to maturing dendritic cells via the DEC-205 receptor improves T cell vaccination, J. Exp. Med. 199 (2004) 815–824.
[8] P.J. Tacken, I.J. de Vries, K. Gijzen, B. Joosten, D. Wu, R.P. Rother, S.J. Faas, C.J. Punt, R. Torensma, G.J. Adema, C.G. Figdor, Effective induction of naive and recall T-cell responses by targeting antigen to human dendritic cells via a humanized anti-DC-SIGN antibody, Blood 106 (2005) 1278–1285.
[9] T. Keler, V. Ramakrishna, M.W. Fanger, Mannose receptor-targeted vaccines, Expert Opin. Biol. Ther. 4 (2004) 1953–1962.
[10] D.I. Bernstein, The skin prick test: "more than meets the eye", Ann. Allergy Asthma Immunol. 92 (2004) 587–588.
[11] A.P. Williams, M.T. Krishna, A.J. Frew, The safety of immunotherapy, Clin. Exp. Allergy 34 (2004) 513–514.
[12] R. Pawankar, G.W. Canonica, S.T. Holgate, R.F. Lockey, WAO White Book on Allergy, 2011.
[13] C.L. Sokol, G.M. Barton, A.G. Farr, R. Medzhitov, A mechanism for the initiation of allergen-induced T helper type 2 responses, Nat. Immunol. 9 (2008) 310–318.
[14] D. Mislovicova, J. Masarova, J. Svitel, R. Mendichi, L. Soltes, P. Gemeiner, B. Danielsson, Neoglycoconjugates of mannan with bovine serum albumin and their interaction with lectin concanavalin A, Bioconjug. Chem. 13 (2002) 136–142.
[15] M. Dubois, K. Gilles, J.K. Hamilton, P.A. Rebers, F. Smith, A colorimetric method for the determination of sugars, Nature 168 (1951) 167.
[16] S.E. Harding, K. Jumel, Light scattering, Current protocols in protein science/editorial board, John E. Coligan … [et al.], Chapter 7 (2001) Unit 7 8.
[17] A. Hartl, R. Weiss, R. Hochreiter, S. Scheiblhofer, J. Thalhamer, DNA vaccines for allergy treatment, Methods 32 (2004) 328–339.
[18] M.N. Torrero, D. Larson, M.P. Hubner, E. Mitre, CD200R surface expression as a marker of murine basophil activation, Clin. Exp. Allergy 39 (2009) 361–369.
[19] A. Stoecklinger, I. Grieshuber, S. Scheiblhofer, R. Weiss, U. Ritter, A. Kissenpfennig, B. Malissen, N. Romani, F. Koch, F. Ferreira, J. Thalhamer, P. Hammerl, Epidermal langerhans cells are dispensable for humoral and cell-mediated immunity elicited by gene gun immunization, J. Immunol. 179 (2007) 886–893.
[20] B.D. Hames, D. Rickwood, Gel Electrophoresis of Nucleic Acids: A Practical Approach (Practical Approach Series), Oxford University Press, 1990.
[21] P.J. Tacken, C.G. Figdor, Targeted antigen delivery and activation of dendritic cells in vivo: steps towards cost effective vaccines, Semin. Immunol. 23 (2011) 12–20.
[22] W.J. Lesterhuis, E.H. Aarntzen, I.J. De Vries, D.H. Schuurhuis, C.G. Figdor, G.J. Adema, C.J. Punt, Dendritic cell vaccines in melanoma: from promise to proof? Crit. Rev. Oncol. Hematol. 66 (2008) 118–134.
[23] I. Caminschi, K. Shortman, Boosting antibody responses by targeting antigens to dendritic cells, Trends Immunol. 33 (2012) 71–77.
[24] K. Drickamer, C-type lectin-like domains, Curr. Opin. Struct. Biol. 9 (1999) 585–590.
[25] H.A. Vaughan, D.W. Ho, V. Karanikas, M.S. Sandrin, I.F. McKenzie, G.A. Pietersz, The immune response of mice and cynomolgus monkeys to macaque mucin 1-mannan, Vaccine 18 (2000) 3297–3309.
[26] B.E. Loveland, A. Zhao, S. White, H. Gan, K. Hamilton, P.X. Xing, G.A. Pietersz, V. Apostolopoulos, H. Vaughan, V. Karanikas, P. Kyriakou, I.F. McKenzie, P.L. Mitchell, Mannan-MUC1-pulsed dendritic cell immunotherapy: a phase I trial in patients with adenocarcinoma, Clin. Cancer Res. 12 (2006) 869–877.
[27] V. Karanikas, L.A. Hwang, J. Pearson, C.S. Ong, V. Apostolopoulos, H. Vaughan, P.X. Xing, G. Jamieson, G. Pietersz, B. Tait, R. Broadbent, G. Thynne, I.F. McKenzie, Antibody and T cell responses of patients with adenocarcinoma immunized with mannan-MUC1 fusion protein, J. Clin. Invest. 100 (1997) 2783–2792.
[28] B. Chackerian, P. Lenz, D.R. Lowy, J.T. Schiller, Determinants of autoantibody induction by conjugated papillomavirus virus-like particles, J. Immunol. 169 (2002) 6120–6126.
[29] A.S. Rosenberg, Effects of protein aggregates: an immunologic perspective, AAPS J. 8 (2006) E501–E507.
[30] M.C. Tan, A.M. Mommaas, J.W. Drijfhout, R. Jordens, J.J. Onderwater, D. Verwoerd, A.A. Mulder, A.N. van der Heiden, D. Scheidegger, L.C. Oomen, T.H. Ottenhoff, A. Tulp, J.J. Neefjes, F. Koning, Mannose receptor-mediated uptake of antigens strongly enhances HLA class II-restricted antigen presentation by cultured dendritic cells, Eur. J. Immunol. 27 (1997) 2426–2435.
[31] A. O'Garra, G. Trinchieri, Are dendritic cells afraid of commitment? Nat. Immunol. 5 (2004) 1206–1208.
[32] L.S. van Rijt, B.N. Lambrecht, Dendritic cells in asthma: a function beyond sensitization, Clin. Exp. Allergy 35 (2005) 1125–1134.
[33] R. Maldonado-Lopez, M. Moser, Dendritic cell subsets and the regulation of Th1/Th2 responses, Semin. Immunol. 13 (2001) 275–282.

[34] B. Pulendran, J.L. Smith, G. Caspary, K. Brasel, D. Pettit, E. Maraskovsky, C.R. Maliszewski, Distinct dendritic cell subsets differentially regulate the class of immune response in vivo, Proc. Natl. Acad. Sci. U. S. A. 96 (1999) 1036–1041.
[35] B.N. Lambrecht, M. De Veerman, A.J. Coyle, J.C. Gutierrez-Ramos, K. Thielemans, R.A. Pauwels, Myeloid dendritic cells induce Th2 responses to inhaled antigen, leading to eosinophilic airway inflammation, J. Clin. Invest. 106 (2000) 551–559.
[36] H. Kuipers, D. Hijdra, V.C. De Vries, H. Hammad, J.B. Prins, A.J. Coyle, H.C. Hoogsteden, B.N. Lambrecht, Lipopolysaccharide-induced suppression of airway Th2 responses does not require IL-12 production by dendritic cells, J. Immunol. 171 (2003) 3645–3654.
[37] H. Kuipers, C. Heirman, D. Hijdra, F. Muskens, M. Willart, S. van Meirvenne, K. Thielemans, H.C. Hoogsteden, B.N. Lambrecht, Dendritic cells retrovirally overexpressing IL-12 induce strong Th1 responses to inhaled antigen in the lung but fail to revert established Th2 sensitization, J. Leukoc. Biol. 76 (2004) 1028–1038.
[38] M.E. Luca, J.M. Kel, W. van Rijs, J. Wouter Drijfhout, F. Koning, L. Nagelkerken, Mannosylated PLP(139–151) induces peptide-specific tolerance to experimental autoimmune encephalomyelitis, J. Neuroimmunol. 160 (2005) 178–187.
[39] L. Bonifaz, D. Bonnyay, K. Mahnke, M. Rivera, M.C. Nussenzweig, R.M. Steinman, Efficient targeting of protein antigen to the dendritic cell receptor DEC-205 in the steady state leads to antigen presentation on major histocompatibility complex class I products and peripheral CD8+ T cell tolerance, J. Exp. Med. 196 (2002) 1627–1638.
[40] D. Hawiger, K. Inaba, Y. Dorsett, M. Guo, K. Mahnke, M. Rivera, J.V. Ravetch, R.M. Steinman, M.C. Nussenzweig, Dendritic cells induce peripheral T cell unresponsiveness under steady state conditions in vivo, J. Exp. Med. 194 (2001) 769–779.
[41] N. Mothes, M. Heinzkill, K.J. Drachenberg, W.R. Sperr, M.T. Krauth, Y. Majlesi, H. Semper, P. Valent, V. Niederberger, D. Kraft, R. Valenta, Allergen-specific immunotherapy with a monophosphoryl lipid A-adjuvanted vaccine: reduced seasonally boosted immunoglobulin E production and inhibition of basophil histamine release by therapy-induced blocking antibodies, Clin. Exp. Allergy 33 (2003) 1198–1208.
[42] O. Talay, D. Yan, H.D. Brightbill, E.E. Straney, M. Zhou, E. Ladi, W.P. Lee, J.G. Egen, C.D. Austin, M. Xu, L.C. Wu, IgE(+) memory B cells and plasma cells generated through a germinal-center pathway, Nat. Immunol. 13 (2012) 396–404.
[43] H. Xiong, J. Dolpady, M. Wabl, M.A. Curotto de Lafaille, J.J. Lafaille, Sequential class switching is required for the generation of high affinity IgE antibodies, J. Exp. Med. 209 (2012) 353–364.
[44] M. Akdis, C.A. Akdis, IgE class switching and cellular memory, Nat. Immunol. 13 (2012) 312–314.
[45] D.R. Wesemann, J.M. Magee, C. Boboila, D.P. Calado, M.P. Gallagher, A.J. Portuguese, J.P. Manis, X. Zhou, M. Recher, K. Rajewsky, L.D. Notarangelo, F.W. Alt, Immature B cells preferentially switch to IgE with increased direct Smu to Sepsilon recombination, J. Exp. Med. 208 (2011) 2733–2746.
[46] B. He, X. Qiao, P.J. Klasse, A. Chiu, A. Chadburn, D.M. Knowles, J.P. Moore, A. Cerutti, HIV-1 envelope triggers polyclonal Ig class switch recombination through a CD40-independent mechanism involving BAFF and C-type lectin receptors, J. Immunol. 176 (2006) 3931–3941.
[47] G. Senti, S. von Moos, F. Tay, N. Graf, T. Sonderegger, P. Johansen, T.M. Kundig, Epicutaneous allergen-specific immunotherapy ameliorates grass pollen-induced rhinoconjunctivitis: a double-blind, placebo-controlled dose escalation study, J. Allergy Clin. Immunol. 129 (2012) 128–135.
[48] G. Senti, N. Graf, S. Haug, N. Ruedi, S. von Moos, T. Sonderegger, P. Johansen, T.M. Kundig, Epicutaneous allergen administration as a novel method of allergen-specific immunotherapy, J. Allergy Clin. Immunol. 124 (2009) 997–1002.